CONF-9011211--2

DE91 014255

# FISSION PRODUCT RETENTION IN TRISO COATED $UO_2$ PARTICLE FUELS SUBJECTED TO HTR SIMULATED CORE HEATING TESTS

C. A. Baldwin and M. J. Kania

Oak Ridge National Laboratory
Oak Ridge, Tennessee, USA

## DISCLAIMER



A paper presented at the:

INTERNATIONAL ATOMIC ENERGY AGENCY
Specialists Meeting on
Behaviour of Gas Cooled Reactor Fuel Under Accident Conditions
Oak Ridge, Tennessee, USA
November 5-7, 1990

# FISSION PRODUCT RETENTION IN TRISO COATED $UO_2$ PARTICLE FUELS SUBJECTED TO HTR SIMULATED CORE HEATING TESTS*

C. A. Baldwin and M. J. Kania

## ABSTRACT

Results of the examination and analysis of 25,730 individual microspheres from spherical fuel elements HFR-K3/1 and HFR-K3/3 are reported. The parent spheres were irradiated in excess of end-of-life exposure and subsequently subjected to simulated core heating tests in a special high-temperature furnace at Forschungszentrum, Jülich, GmbH. (KFA). Following the heating tests, the spheres were electrolytically deconsolidated to obtain unbonded fuel particles for Irradiated Microsphere Gamma Analyzer (IMGA) analysis.

For sphere HFR-K3/1, which was heated for 500 h at 1600°C, only four particles were identified as having released fission products. The remaining particles from the sphere showed no statistical evidence of fission product release. Scanning Electron Microscopy (SEM) examination showed that three of the defect particles had large sections of the TRISO coating missing, while the fourth appeared normal.

For sphere HFR-K3/3, which was heated for 100 h at 1800°C, the IMGA data revealed that fission product release (cesium) from individual particles was significant and that there was large particle-to-particle variation in retention capabilities. Individual particle release (cesium) averaged ten times the KFA-measured integral spherical fuel element release value. In addition, the bimodal distribution of the individual particle data indicated that two distinct modes of failure at fuel temperatures of 1800°C and above may exist.

## 1. INTRODUCTION

Unbonded coated particles (microspheres) from two irradiated spherical fuel elements have been examined using the IMGA system. The examinations were conducted under the U.S.-Federal Republic of Germany (FRG) Umbrella Agreement on High-Temperature Reactor (HTR) Development, Project Work Statement FD-20. The postirradiation examination work performed at Oak Ridge National Laboratory (ORNL) provided statistically significant detailed data on fuel failure fraction,

---

*Research sponsored by the Office of Advanced Reactor Programs, Division of HTGRs, U. S. Department of Energy, under contract DE-AC05-84OR21400 with Martin Marietta Energy Systems, Inc.

quantification of fission product retention, and identification of released species. The examination method of primary interest is the IMGA system, and together with analytic tools developed at ORNL, it represents a unique system for characterizing the performance of a large population of HTR coated-particle fuels with statistical significance.

This paper summarizes results obtained from examining and analyzing 25,730 individual microspheres taken from two spherical fuel elements. The coated particles making up these spheres were FRG reference low enriched uranium (LEU) $UO_2$ TRISO coated particles, and they, along with the spherical fuel elements, were fabricated to HTR-Modul quality specifications by the FRG HTR fuel manufacturer HOBEG, GmbH.

The HFR-K3 experiment assembly, specifically designed to test HTR spherical fuel elements, was irradiated in the High Flux Reactor (HFR) located at Petten, the Netherlands.[1] The assembly contained three separate compartments, each with an independent sweep gas and temperature control system. Sphere HFR-K3/1 was irradiated in the upper compartment at an operating temperature ranging from 1020°C to 1200°C and accumulated a fast neutron fluence of $4.0 \times 10^{25}$ neutrons/$m^2$ ($E \geq 0.1$ MeV). Spheres HFR-K3/2 and HFR-K3/3 were irradiated in the central compartment at an operating temperature ranging from 700°C to 920°C and accumulated fast neutron fluences of $5.8 \times 10^{25}$ and $5.9 \times 10^{25}$ neutrons/$m^2$ ($E \geq 0.1$ MeV), respectively. Sphere HFR-K3/4 was irradiated in the lower compartment at an operating temperature ranging from 1020°C to 1220°C and accumulated a fast neutron fluence of $4.9 \times 10^{25}$ neutrons/$m^2$ ($E \geq 0.1$ MeV). After 359 full-power days in the HFR at a nominal 45-MW power level, the experiment was discharged from the reactor. At that time, spheres 1 through 4 had achieved average burnups of 7.5%, 10.0%, 10.6%, and 9.0% fissions per initial heavy metal atom (FIMA), respectively.

Following irradiation, the experiment was disassembled and the major components shipped to KFA for postirradiation examination. After the fuel spheres were recovered from their respective compartments, spheres HFR-K3/2 and HFR-K3/4 were placed in long-term storage and spheres HFR-K3/1 and HFR-K3/3 were subjected to simulated core heating tests in a specially designed high-temperature furnace located in the hot cells at KFA.[2] Sphere HFR-K3/1 was tested for 500 h at 1600°C, and sphere HFR-K3/3 was tested for a total of 100 h at 1800°C. The latter test consisted of two separate runs of 25 h and 75 h. During the tests, the fission products released from the spheres were collected and analyzed. The gaseous species were collected in activated charcoal cold traps, and the metallic species were collected on a removable deposition surface (condensate plates) placed in the high-temperature furnace.

Following the simulated core heating tests, the spheres were electrolytically deconsolidated to obtain unbonded fuel particles for IMGA analysis. In the deconsolidation process, the outer circumference of a sphere was removed first,

leaving a cylinder approximately 2 cm in diameter. During the second part of the process, the cylinder was upended and lowered into the electrolyte in ten discrete steps. After each deconsolidation step, the unbonded particles were collected and packaged separately. Thus, for each sphere, 11 samples of unbonded particles were obtained, with 10 of the samples providing a profile of fuel from the edge through the center of the sphere. Figure 1 illustrates the approximate location of the samples in the original spherical element.

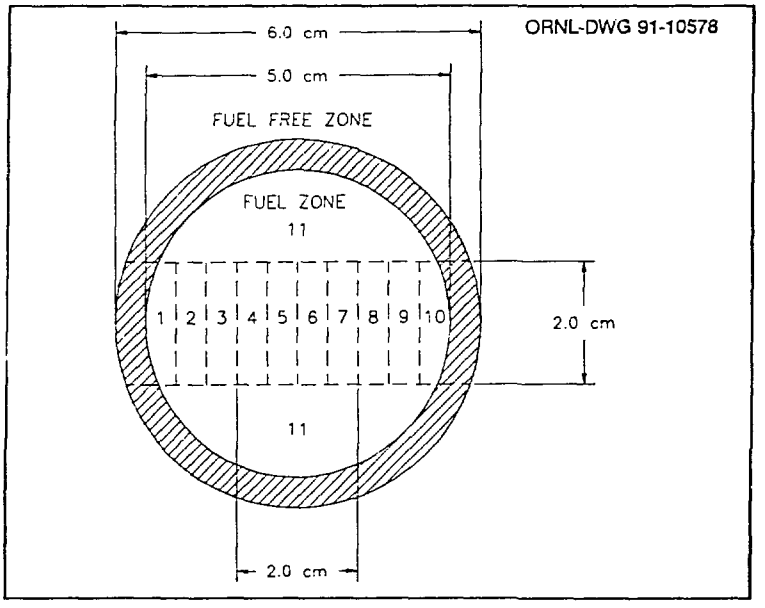


Fig. 1. Profile disintegration of FRG spherical fuel element.

The IMGA system is a unique research tool located in the Irradiated Fuels Examination Laboratory (IFEL) at ORNL.[3] The primary function of the IMGA system is to accurately measure radioisotopic inventories of individual coated particles used in HTR applications. This is accomplished by detecting the gamma radiation given off by the fuel particles as various fission products decay. The system consists of three major components: (1) a high-resolution gamma-ray spectrometer, (2) a computer-based multichannel analyzer, and (3) an automated particle-handling system. These three components have been integrated into a sophisticated system capable of autonomous operation. During initial test examinations of particles from spheres HFR-K3/1 and HFR-K3/3, a problem was encountered. The design of the IMGA particle handler will allow only those particles with a diameter less than 1250 $\mu$m to be safely transported. The nominal diameter of the particles from the HFR-K3 spheres was about 920 $\mu$m; however, some of the particles retained the porous matrix

graphite overcoating, which increased the diameter to about 1320 $\mu$m. Normally the overcoating is removed during the electrolytic deconsolidation process, but in the HFR-K3 spheres a significant fraction of the particles from the central cylinder retained their overcoatings.

It is not known if the postirradiation core heating test caused the problem or whether there was some abnormality in the deconsolidation process. In any event, it was necessary to remove the overcoated particles before the samples could be examined by IMGA. This was accomplished by using several wire sieves to grade the unbonded particles by size. Approximately 1% of the particles from the outer circumference samples and 40% of the particles from the central cylinder samples retained their overcoatings. These particles were set aside, and only the clean particles that remained were examined. A SEM photograph illustrating a particle with a portion of its overcoating intact is shown in Fig. 2.

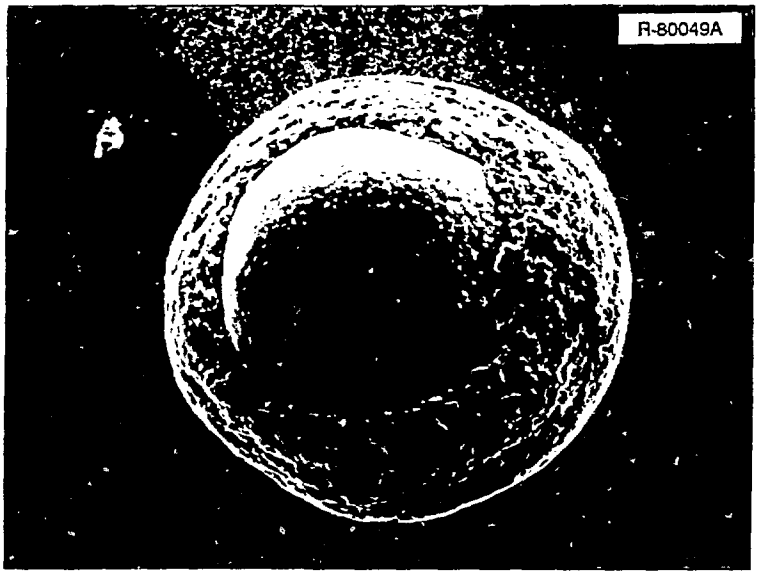


Fig. 2. SEM photograph (50X) of a particle which has retained a portion of the matrix graphite overcoating.

## 2. FISSION PRODUCT RETENTION ANALYSIS

All particles free of overcoating material from the two HFR-K3 spheres were examined by the IMGA system. This represents 13,750 fuel particles from sphere HFR-K3/1 and 11,980 fuel particles from sphere HFR-K3/3. Of the 13,750 individual particles examined from sphere HFR-K3/1, four were identified as having peculiar characteristics and were segregated by the IMGA system. SEM photographs of these four particles are shown in Fig. 3, and their fission product inventories are given in

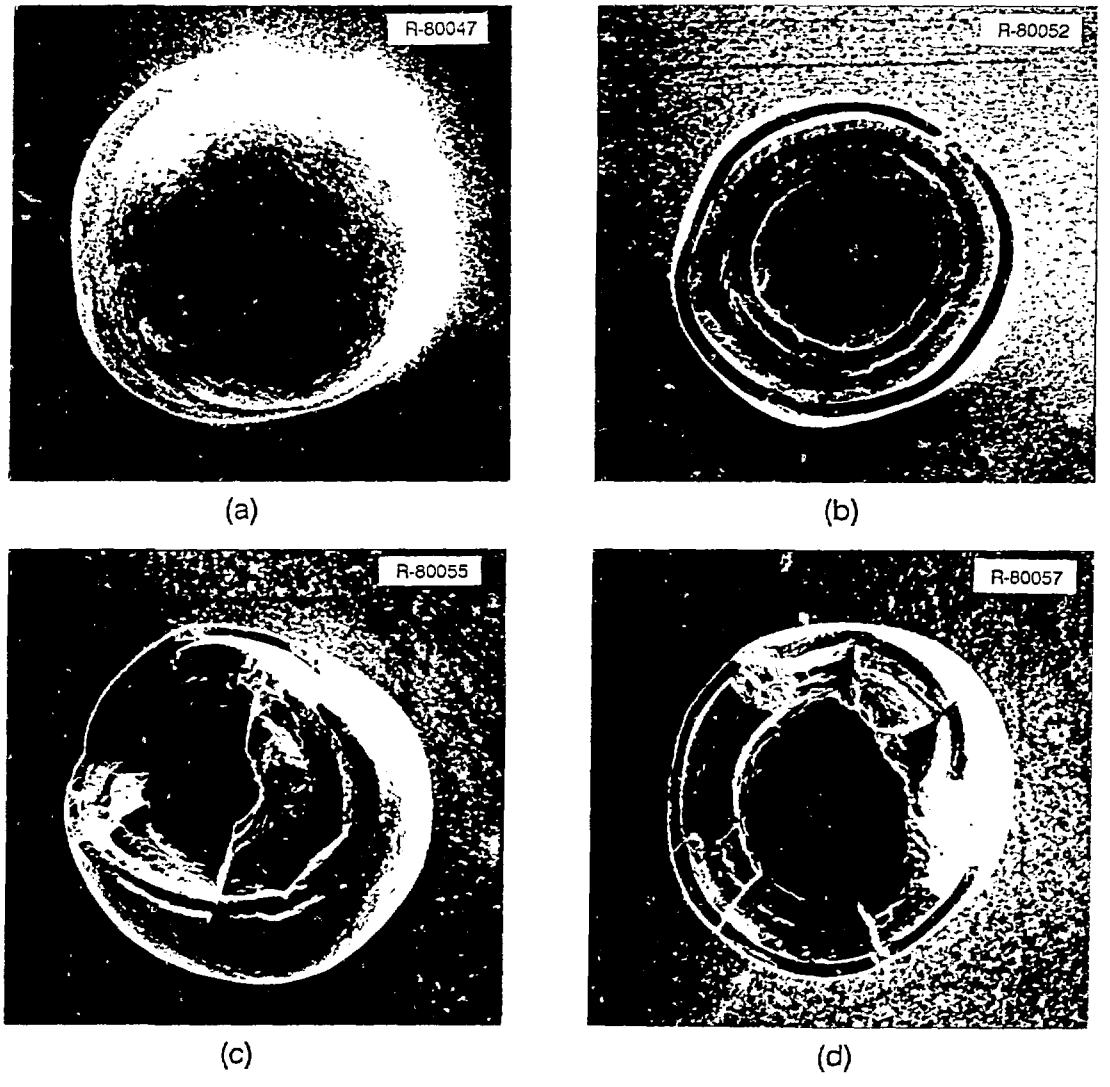


Fig. 3. SEM photographs (50X) of selected particles from sphere HFR-K3/1.

Table 1. From the visible and analytical evidence, particles 3(b) through 3(d) appear to be TRISO coating fragments. Visual and analytical evidence for particle 3(a), however, is inconclusive and somewhat contradictory. Although the particle appears intact, its $^{106}Ru$:$^{144}Ce$ activity ratio is very low, usually indicating some loss of kernel material. For the HFR-K3/3 sphere, no visibly defective particles were found; however, analysis of mean activities and activity ratios revealed that essentially all particles from the sphere exhibited fission product release (cesium).

Table 1. Fission product activities for four particles isolated during the examination of sphere HFR-K3/1 [a]

| Particle | $^{106}Ru$ (622 keV) (Bq) | $^{134}Cs$ (604 keV) (Bq) | $^{137}Cs$ (662 keV) (Bq) | $^{144}Ce$ (133 keV) (Bq) | $^{154}Eu$ (1274 keV) (Bq) |
|---|---|---|---|---|---|
| 3(a) Unknown | 1.80E+07 | 1.03E+06 | 1.28E+06 | 2.03E+07 | 4.98E+04 |
| 3(b) Fragment | 1.22E+07 | 4.98E+06 | 3.85E+06 | ND | 3.21E+02 |
| 3(c) Fragment | 7.07E+06 | 3.83E+06 | 2.96E+06 | ND | ND |
| 3(d) Fragment | ND[b] | 2.26E+06 | 1.68E+06 | ND | 2.16E+03 |
| *Sphere Means*[c] | *2.31E+07* | *5.45E+06* | *4.82E+06* | *9.14E+07* | *1.57E+05* |

[a] Activities corrected to September 5, 1983.

[b] ND - none detected.

[c] Sphere means are based on the analysis of 13,746 individual particle records.

To determine how much of a given fission or activation product a particle has retained, it is necessary to know the inventory that should be present in the particle assuming nothing has escaped. Normally such information requires detailed calculations of the buildup, decay, and burnup of individual isotopes during the irradiation period and subsequent out-of-reactor hold-time for the fuel. Unfortunately, for the HFR-K3 spheres, such detailed calculations were not available. As an approximation, the following assumption was made: during irradiation no loss of fission or activation products occurred from the spheres. This assumption is supported by the end-of-life (EOL) fission gas release rate vs birth rate (R/B) values for the spheres. These values indicate that the EOL $^{85m}Kr$ R/B was less than $2 \times 10^{-7}$.

Using a gas release value for a failed $UO_2$ particle [$(R/B)_i$] of about $5x10^{-3}$, the EOL capsule R/B data represent a $\leq 4x10^{-5}$ failed particle fraction. Approximately 16,400 particles were contained in each spherical fuel element, so this activity represents <66% of a single particle inventory. Therefore, the activity must be due to the heavy metal contaminations present in the sphere from fabrication. The low EOL R/B data are representative of no failed $UO_2$ particles.

If no particles released fission products during irradiation, then coupled measurements and calculations performed at KFA on the fuel sphere before it was subjected to the simulated core heating test can be used to estimate mean particle activities at EOL. Mean values were obtained by dividing the sphere total activities reported by KFA[4] by 16,400 particles per sphere. Note that two sets of data were reported by KFA for the sphere and in most instances were in close agreement. The exception was the activity for $^{144}Ce$, where a discrepancy of approximately 15% exists between the measured and the calculated values. Because of their good agreement with IMGA measurements the higher calculated values were used. Cerium in oxide kernels is known to form stable compounds even at high temperatures. The cerium inventories measured with IMGA are the most representative of the actual particle inventory, because they are direct measurements performed on several thousand particles. Tables 2 and 3 compare mean particle activities before and after the HFR-K3 spheres were subjected to the simulated core heating tests.

Table 2. Comparison of mean particle activities before and after heating sphere HFR-K3/1 for 500 h at 1600°C [a]

| | After 500 h @ 1600°C[b] | | | Before heating[c] | | |
|---|---|---|---|---|---|---|
| Isotope | Photon (keV) | Particle mean (Bq) | Std.Dev. (%) | Sphere total (Bq) | Particle mean (Bq) | After / Before |
| $^{106}Ru$ | 622 | 2.31E+07 | 11.81 | 3.64E+11 | 2.22E+07 | 1.04 |
| $^{134}Cs$ | 604 | 5.45E+06 | 9.95 | 9.21E+10 | 5.62E+06 | 0.97 |
| $^{137}Cs$ | 662 | 4.82E+06 | 6.12 | 8.86E+10 | 5.40E+06 | 0.89 |
| $^{144}Ce$ | 133 | 9.14E+07 | 7.46 | 1.52E+12 | 9.27E+07 | 0.99 |
| $^{154}Eu$ | 1274 | 1.57E+05 | 10.99 | 2.86E+09 | 1.74E+05 | 0.90 |

[a] Activities corrected to September 5, 1983.
[b] Based on measurements of 13,746 particles at ORNL.
[c] Based on measurement of the entire sphere at KFA.

Table 3. Comparison of mean particle activities before and after heating sphere HFR-K3/3 for 100 h at 1800°C [a]

| Isotope | After 100 h @ 1800°C[b] | | | Before heating[c] | | After / Before |
|---|---|---|---|---|---|---|
| | Photon (keV) | Particle mean (Bq) | Std.Dev. (%) | Sphere total (Bq) | Particle mean (Bq) | |
| $^{106}$Ru | 622 | 4.00E+07 | 8.91 | 6.14E+11 | 3.74E+07 | 1.07 |
| $^{134}$Cs | 604 | 4.59E+06 | 51.99 | 1.81E+11 | 1.10E+07 | 0.42 |
| $^{137}$Cs | 662 | 2.84E+06 | 52.61 | 1.19E+11 | 7.26E+06 | 0.39 |
| $^{144}$Ce | 133 | 1.19E+08 | 6.41 | 1.91E+12 | 1.16E+08 | 1.03 |
| $^{154}$Eu | 1274 | 2.89E+05 | 7.56 | 5.24E+09 | 3.20E+05 | 0.90 |

[a] Activities corrected to September 5, 1983.
[b] Based on measurements of 11,980 particles at ORNL.
[c] Based on measurement of the entire sphere at KFA.

The comparison indicates a sphere total release (cesium) for sphere HFR-K3/1 of approximately 5 to 10%. For sphere HFR-K3/3, the comparison indicates a sphere total release (cesium) of approximately 60%. Cesium escaping the individual microspheres should be retained in the matrix graphite or detected leaving the spherical element by the condensate plates placed in the high-temperature furnace. Table 4 summarizes integral release data for the condensate plates and the matrix graphite for the two spheres as reported by KFA[5] and by Harwell Laboratory, England[6]. For the HFR-K3/1 sphere, less than 0.2% of the initial cesium inventory was detected, and for the HFR-K3/3 sphere, less than 15% was detected. Thus, a mass balance analysis fails to confirm the release of cesium implied by the ratios in Tables 2 and 3.

If one assumes that individual particle failures are responsible for the release of fission products in the spherical elements, then it should be possible to distinguish these particles from a distribution of non-failed particles. For the purpose of this analysis, particle failure is defined as a significant release of fission products. A simple histogram method was employed to analyze the individual particle data. First, activity ratios for each particle were computed to take into account the variable masses of the individual particles. To provide a consistent basis for comparison the ratios were then normalized to the KFA preheating test values. The histogram representation of the particle data was then obtained by defining intervals which were 2% wide and

Table 4. Fraction of cesium released to matrix graphite and condensate plates for spheres HFR-K3/1 and HFR-K3/3

| Sphere | Isotope | HARWELL | | KFA | |
|---|---|---|---|---|---|
| | | Matrix graphite | Condensate plate | Matrix graphite | Condensate plate |
| HFR-K3/1 | $^{134}Cs$ | 1.6E-03 | 1.4E-04 | - | 1.3E-04 |
| | $^{137}Cs$ | 1.8E-03 | 1.2E-04 | 1.2E-03 | 1.1E-04 |
| HFR-K3/3 | $^{134}Cs$ | 8.7E-02 | 1.2E-01 | - | 6.4E-02 |
| | $^{137}Cs$ | 9.7E-02 | 1.3E-01 | 8.2E-02 | 5.9E-02 |

counting the number of normalized ratios which fell within a given interval. The histograms are shown in Figs. 4 through 6 for the ratios $^{106}Ru$:$^{144}Ce$, $^{137}Cs$:$^{144}Ce$, and $^{154}Eu$:$^{144}Ce$, respectively. In the figures, the particle data (vertical bars) have been superimposed over a theoretical normal distribution (gray) that was calculated by using the mean and standard deviation of the experimental distribution. The particle data have also been divided into two groups representing the exterior and interior of a sphere. The exterior group is composed of particle data from samples 1 through 3 and samples 8 through 11. The interior group is composed of particle data from samples 4 through 7 (see Fig. 1).

Figure 4 shows the distribution of $^{106}Ru$:$^{144}Ce$ ratios for the two spheres. Note that for sphere HFR-K3/1, the four particles shown in Figs. 3(a) through 3(d) were removed from the analysis because their $^{144}Ce$ inventories were either too low or below detection limits. Aside from these four particles, examination of the individual particle data revealed no particles with abnormally high or low ratios for either sphere. This fact, along with the good absolute agreement with KFA preheating test data for $^{106}Ru$ and $^{144}Ce$, supports the assertion that all particles in the main distributions have retained their $^{106}Ru$ and $^{144}Ce$ inventories. A comparison of interior vs exterior particles reveals that particles from the sphere interior have on average lower ratios. This is probably due to differences in fuel burnup caused by thermal neutron self-shielding.

Figure 5 shows the distribution of $^{137}Cs$:$^{144}Ce$ ratios for the two spheres. This ratio is generally the most useful for detecting particle failure because the cesium species are mobile and move relatively quickly through pyrocarbon and defective SiC coatings at accident simulation temperatures. Failed particles typically constitute a separate peak in the overall distribution due to the accelerated loss of cesium. For the HFR-K3/1 sphere, no particles with abnormally low ratios were observed

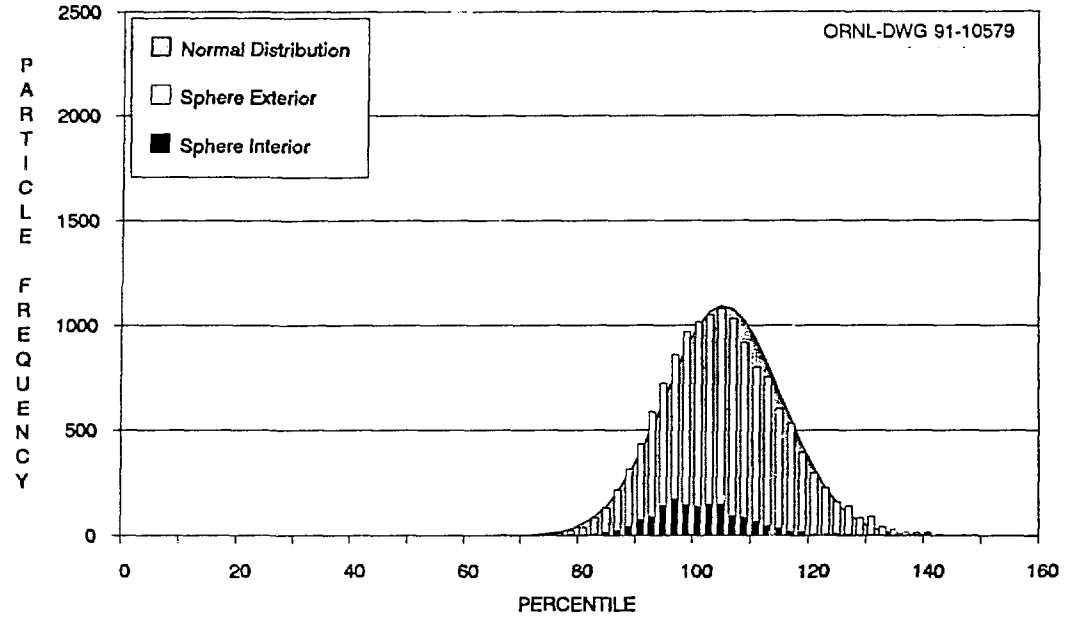


(a)

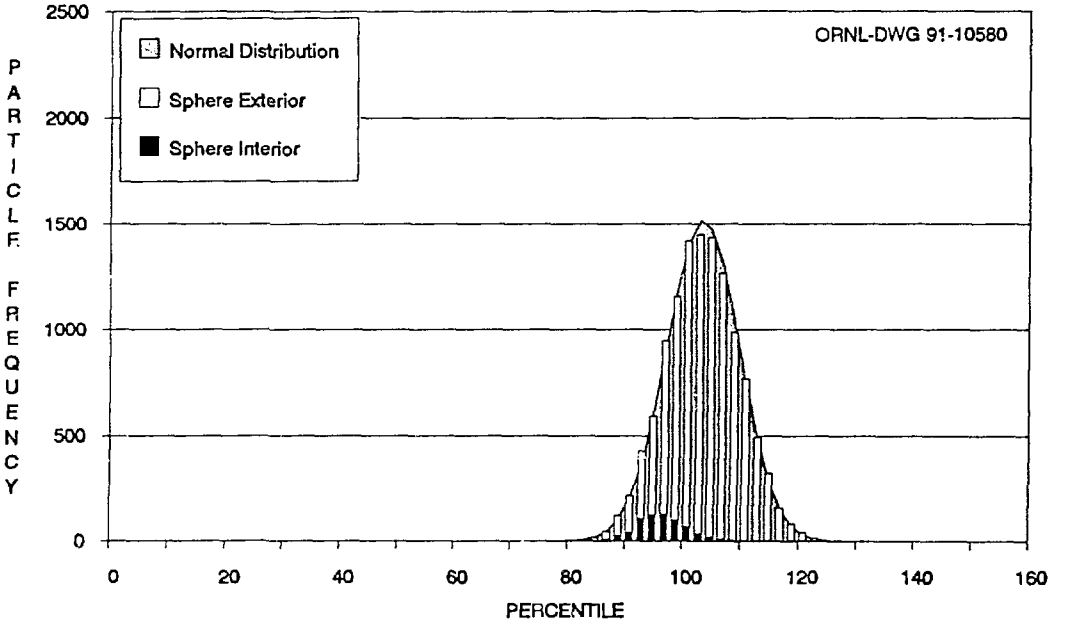


(b)

Fig. 4. Distribution of $^{106}Ru$:$^{144}Ce$ ratios normalized to KFA preheating test values for (a) sphere HFR-K3/1 and (b) sphere HFR-K3/3. For comparison a normal distribution based on the experimental data is plotted in the background.

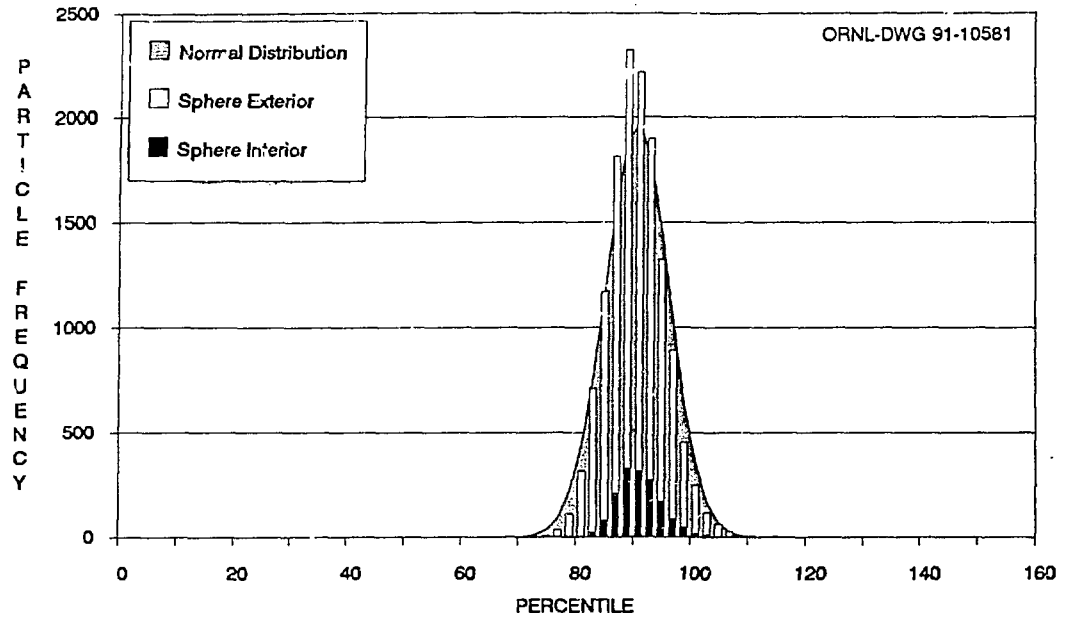


(a)

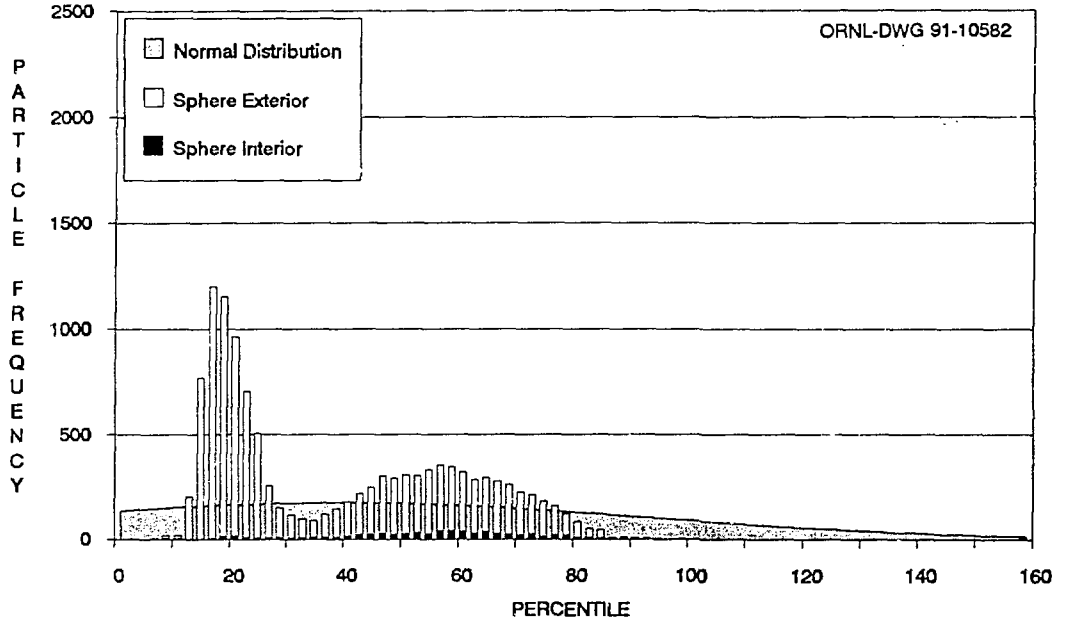


(b)

Fig. 5. Distribution of $^{137}Cs$:$^{144}Ce$ ratios normalized to KFA preheating test values for (a) sphere HFR-K3/1 and (b) sphere HFR-K3/3. For comparison a normal distribution based on the experimental data is plotted in the background.

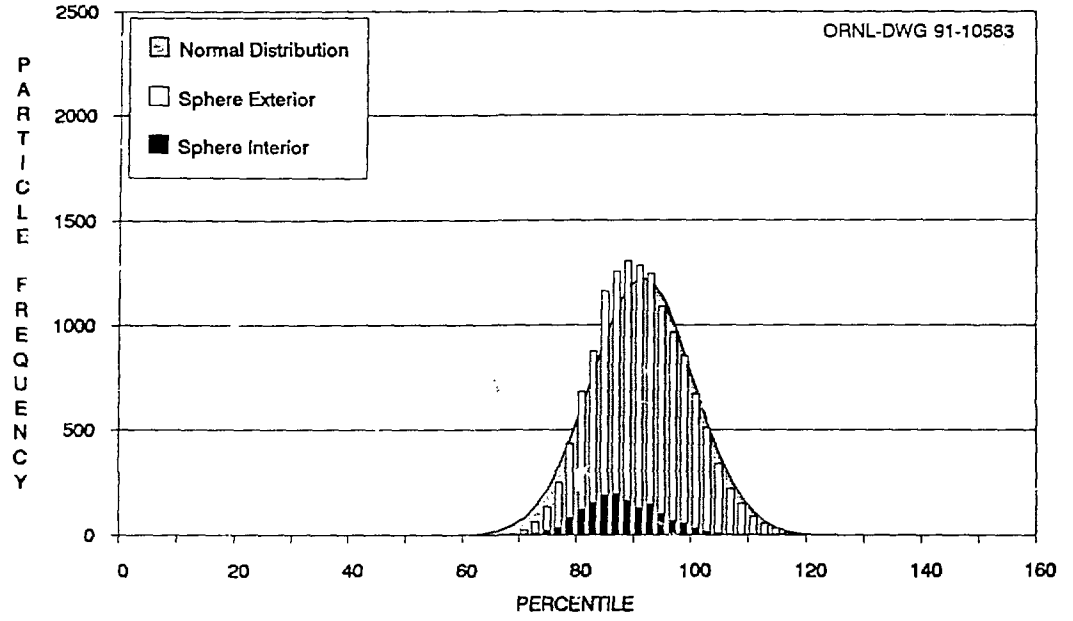


(a)

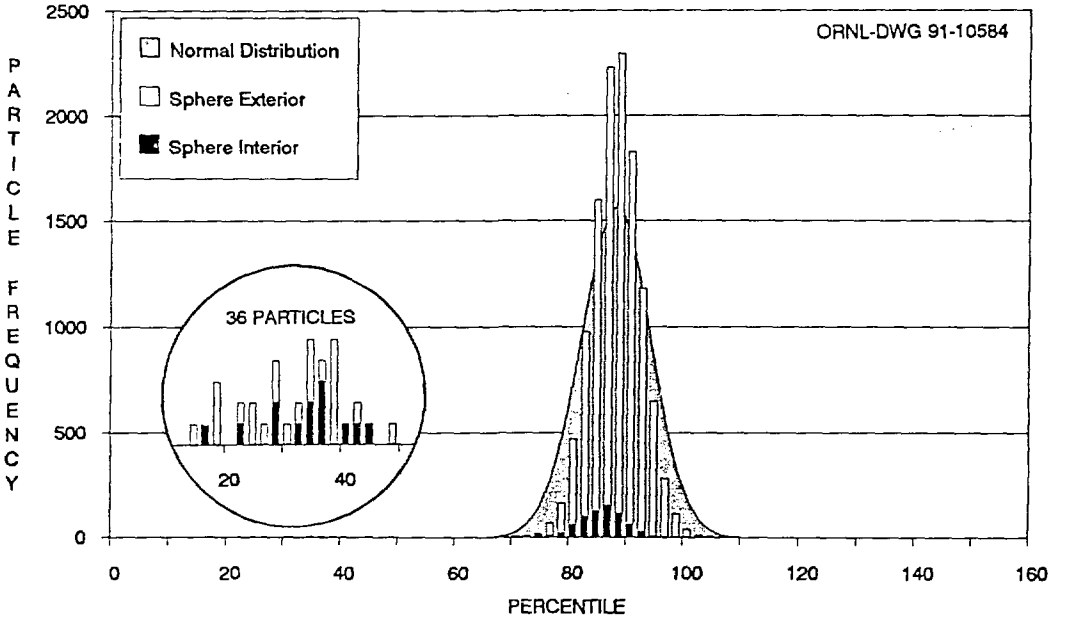


(b)

Fig. 6. Distribution of $^{154}Eu$:$^{144}Ce$ ratios normalized to KFA preheating test values for (a) sphere HFR-K3/1 and (b) sphere HFR-K3/3. For comparison a normal distribution based on the experimental data is plotted in the background.

(excluding the four particles discussed earlier). For sphere HFR-K3/3, however, there appear to be two distributions of particles which overlap, each containing approximately half of the particles from the sphere. Both distributions are centered significantly lower than the 100 percentile; thus these distributions probably represent particles with high- and medium-release characteristics. In other words, for sphere HFR-K3/3, there is no identifiable distribution of non-failed particles based on cesium release. The data indicate that individual particle release for cesium varies from approximately 10% to as much as 90% of the mean particle inventory. Although difficult to discern in Fig. 5(b), 54% of the particles from the sphere exterior fall into the high release distribution while only 13% of the particles from the sphere interior fall into this distribution. On average, particles from the exterior exhibited higher cesium release than particles from the interior.

Figure 6 shows the distribution of $^{154}Eu$:$^{144}Ce$ ratios for the two spheres. Again, for sphere HFR-K3/1, no particles with abnormally low ratios were observed (excluding the four particles discussed earlier). For sphere HFR-K3/3, however, there appear to be two well-defined distributions of particles. The smaller distribution contains 36 particles with low ratios, and the larger distribution contains the balance of the particles from the sphere. These data suggest that europium is less mobile than cesium but will move through pyrocarbon and defective SiC coatings at higher temperatures. Other than a slight burnup effect, there appears to be no significant difference in behavior between sphere interior and sphere exterior particles.

## 3. CONCLUSION

Postirradiation examination of 25,730 microspheres taken from two FRG spherical fuel elements by the IMGA system has been completed . This represents the greatest number of individual particles from a single experiment ever analyzed by the system. The parent spheres from which the unbonded particles were obtained exceeded normal end-of-life irradiation conditions and were subsequently subjected to simulated core heating tests in a special high-temperature furnace at KFA. The testing consisted of heating spherical element HFR-K3/1 for 500 h at 1600°C and spherical element HFR-K3/3 for 100 h at 1800°C. After the heating test, the spheres were electrolytically deconsolidated to obtain unbonded fuel particles for IMGA examination.

During the irradiation period in the HFR, the fission gas R/B was monitored. The EOL R/B data support the assumption that no particles in the spheres failed during the irradiation period. Therefore, coupled measurements and calculations performed on the spheres before the heating test were used to estimate mean particle activities. These preheating test activities were compared directly with IMGA measurements made on the unbonded particles after the heating test.

Although absolute comparisons with KFA preheating test activities indicated some fission product release (cesium) for sphere HFR-K3/1, a mass balance analysis was able to confirm only a small percentage of the loss. In addition, an examination of the distribution of individual particle data revealed no statistical evidence of individual particle failures in the main set of particles. This lack of evidence of individual particle failure does not rule out a uniform loss of cesium from all of the particles examined; however, a uniform loss on the order of 5 to 10% would surely have been detected in the analysis of the condensate plates and matrix graphite. For sphere HFR-K3/3, a significantly higher release of cesium was indicated from the analysis of the individual microspheres than was indicated from the analysis of the matrix graphite and the condensate plates. Individual particle release averaged ten times the KFA-measured integral spherical fuel element release value. The particle data also suggest that there may be two distinct modes of failure at fuel temperatures of 1800°C and above with significant differences in release characteristics.

## REFERENCES


1. R. Gontard, B. Hürttlen, and A. W. Mehner, *HBK-Projekt Hochtemperatur-Reaktor Brennstoff-Kreislauf Vorbestrahlungsbericht für die Experimente HFR-K3(D138.03) und FRJ2-K13(JK13)*, Kernforschungsanlage Jülich GmbH., HBK-IB-4/82, June 1982.

2. H. Nabielek, W. Schenk, W. Heit, A. W. Mehner, and D. T. Goodin, "The Performance of High-Temperature Reactor Fuel Particles at Extreme Temperatures", *Nuclear Technology*, Vol. 84, 62-81, January 1989.

3. K. H. Valentine and M.J. Kania, *IMGA Operating Manual*, Oak Ridge National Laboratory, Oak Ridge, Tennessee, ORNL/TM-6576, August 1979.

4. R. Gontard and H. Nabielek, *Performance Evaluation of Modern HTR TRISO Fuels*, Forschungszentrum Jülich GmbH., HTA-IB-05/90, July 1990, Table 3.2.3.2.

5. W. Schenk and H. Nabielek, *Kugelbrennelemente mit TRISO-Partikeln bei Störfalltemperaturen*, Kernforschungsanlage Jülich GmbH., Jül-Spez-487, January 1989, Tables 61, 97, and 139.

6. P. E. Brown, A. J. Inns, R. J. Pateman, B. A. Phillips, and B. M. Sharpe, *Post-Irradiation Examination of HTR Fuel Elements*, Harwell Laboratory, Didcot, Oxon, England, AERE-G4740, May 1988, Tables 25 and 26.